ELSEVIER

Self-assembly of diorganotin(IV) 2-{[(E)-1-(2-oxyaryl)alkylidene]amino}acetates: An investigation of structures by X-ray diffraction, solution and solid-state tin NMR, and electrospray ionization MS

Tushar S. Basu Baul [a,*], Cheerfulman Masharing [a], Rudolph Willem [b], Monique Biesemans [b], Michal Holčapek [c], Robert Jirásko [c], Anthony Linden [d,*]

[a] Department of Chemistry, North-Eastern Hill University, NEHU Permanent Campus, Umshing, Shillong 793 022, India
[b] High Resolution NMR Centre (HNMR) and Department of Polymer Science and Structural Chemistry, Vrije Universiteit Brussel (VUB), Pleinlaan 2, B-1050 Brussel, Belgium
[c] University of Pardubice, Faculty of Chemical Technology, Department of Analytical Chemistry, nám. Čs. legií 565, 53210 Pardubice, Czech Republic
[d] Institute of Organic Chemistry, University of Zurich, Winterthurerstrasse 190, CH-8057 Zurich, Switzerland

Abstract

The diorganotin(IV) compounds, $[Me_2SnL^2(OH_2)]_2$ (1), $[^nBu_2SnL^2(OH_2)]_2$ (2), $[^nBu_2SnL^1]_3 \cdot 0.5C_3H_6O$ (3), $[^nBu_2SnL^3]_3 \cdot 0.5C_6H_6$ (4) and $[Ph_2SnL^3]_n \cdot 0.5C_6H_6$ (5) (L = carboxylic acid residue, i.e., 2-{[(E)-1-(2-oxyaryl)alkylidene]amino}acetate), were synthesized by treating the appropriate diorganotin(IV) dichloride with the potassium salt of the ligand in anhydrous methanol. The reaction of Ph_2SnL^2 (L = 2-{[(E)-1-(2-oxyphenyl)ethylidene]amino}acetate) with 1,10-phenanthroline (Phen) yielded a 1:1 adduct of composition, $[Ph_2SnL^2(Phen)]$ (6). The crystal structures of 1–6 were determined. The crystal of 1 is composed of centrosymmetric dimers of the basic $Me_2SnL^2(OH_2)$ moiety, where the two Sn-centres are linked by two asymmetric Sn–O···Sn bridges involving the carboxylic acid O atom of the ligand and a long Sn···O distance of 3.174(2) Å. The dimers are further linked into columns by hydrogen bonds. The coordination geometry about the Sn atom is a distorted pentagonal bipyramid with the two methyl groups in axial positions. The structure of 2 is similar. The same Sn atom coordination geometry is observed in compound 3, which is a cyclic trinuclear $[^nBu_2SnL^1]_3$ compound. Each Sn atom is coordinated by the phenoxide O atom, one carboxylate O atom and the imino N atom from one ligand and both the exo- and endo-carboxylate O atoms (mean Sn–O(exo): 2.35 Å; Sn–O(endo): 2.96 Å) from an adjacent ligand to form the equatorial plane, while the two butyl groups occupy axial positions. Compound 4 was found to crystallize in two polymorphic forms. The Sn-complex in both forms has a trinuclear $[^nBu_2SnL^3]_3$ structural motif similar to that found in 3. In compound 5, distorted trigonal bipyramidal Ph_2SnL^3 units are linked into polymeric cis-bridged chains by a weak Sn···O interaction (3.491(2) Å) involving the exocyclic O atom of the tridentate ligand of a neighboring Sn-complex unit. This interaction completes a highly distorted octahedron about the Sn atom, where the weakly coordinated exocyclic O atom and one phenyl group are trans to one another. In contrast, a monomeric distorted pentagonal bipyramidal geometry is found for adduct 6 where the Sn-phenyl groups occupy the axial positions. The solution and solid-state structures are compared by using ^{119}Sn NMR chemical shift data. Compounds 1–6 were also studied using ESI-MS and their positive- and negative-ions mass fragmentation patterns are discussed.
© 2005 Elsevier B.V. All rights reserved.

---

* Corresponding authors. Tel.: +91 364 2722626; fax: +91 364 2550486/2721000 (T.S. Basu Baul); Tel.: +41 44 635 4228; fax: +41 44 635 6812 (A. Linden).
E-mail addresses: basubaul@nehu.ac.in (T.S. Basu Baul), alinden@oci.unizh.ch (A. Linden).

1. Introduction

The increasing interest in organotin carboxylates of substituted benzoic acids in recent years has, to a large extent, been prompted by their new structural diversity [1] and broad therapeutic activity [2]. Recent reports on the structures of organotin complexes [3–7] show that 2-{[(*E*)-1-(2-hydroxyaryl)alkylidene]amino}-acetates (Fig. 1) and related systems are very versatile ligands, which have configurational flexibility, thereby creating the possibility of a variety of coordination modes. The mode of coordination of such tridentate ligands to various organotin-moieties is known [3–7]. In addition, the reaction of diorganotin(IV) complexes of such ligands with R_nSnCl_{4-n} (R = Ph, *n* = 3 and R = ^tBu, *n* = 2) has been shown to involve an unprecedented dinuclear molecular adduct formation, yielding complexes of the form $R_2SnL–R_nSnCl_{4-n}$ where two tin atoms are bridged via the carboxylate O–C–O group of a L ligand [3–7]. In our research programme towards new and better therapeutic agents, we investigated the activity of these compounds *in vivo* in *Ehrlich ascites* carcinoma cells [5]. This class of compounds, in particular the diphenyltin(IV) derivative, has provided exceptionally good *in vitro* antitumour activity against seven well characterized human tumour cell lines, viz., A498 (renal cancer), WIDR (colon cancer), M19 MEL (melanoma), IGROV (ovarian cancer), H226 (non-small cell lung cancer), MCF-7 and EVSA-T (breast cancer), using NCI protocols [8].

In this paper, we report further results concerning organotin–ligand bonding patterns in diorganotin(IV) compounds. The solid-state structures of [Me$_2$Sn-L^2(OH$_2$)]$_2$ (**1**), [$^nBu_2$SnL^2(OH$_2$)]$_2$ (**2**), [$^nBu_2$SnL^1]$_3$·0.5C$_3$-H$_6$O (**3**), [$^nBu_2$SnL^3]$_3$·0.5C$_6$H$_6$ (**4**), [Ph$_2$SnL^3]$_n$·0.5C$_6$H$_6$ (**5**) and Ph$_2$SnL^2(Phen) (**6**) have been determined using single crystal X-ray crystallography in
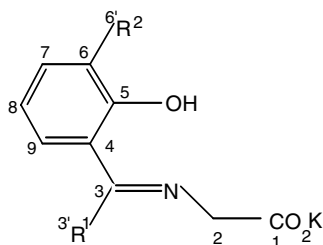
order to elucidate the Sn-coordination. The tin coordination of these complexes in solution has been deduced from ^{119}Sn NMR data recorded using a non-coordinating solvent, while the solid-state ^{117}Sn CP MAS NMR data (where measurements were possible) are correlated with the crystallographic results. In addition, the cleavage of the most labile bond in each molecule has been studied using ESI mass spectroscopy.

2. Experimental

2.1. Materials

The solvents used in the reactions were of AR grade and dried using standard procedures. Benzene was distilled from sodium benzophenone ketyl. Dimethyltin- (Fluka), di-*n*-butyltin- (Merck), diphenyltin- (Aldrich) dichlorides and 1,10-phenanthroline monohydrate (SD Fine chemicals) were used as received.

2.2. Physical measurements

Carbon, hydrogen and nitrogen analyses were performed with a Perkin–Elmer 2400 series II instrument. IR spectra in the range 4000–400 cm^{-1} were obtained on a BOMEM DA-8 FT-IR spectrophotometer with samples run as KBr discs. The ^{1}H, ^{13}C and ^{119}Sn NMR spectra were recorded on a Bruker ACF 300 spectrometer and measured at 300.13, 75.47 and 111.92 MHz, respectively. The ^{1}H, ^{13}C and ^{119}Sn chemical shifts were referenced to Me$_4$Si set at 0.00 ppm, CDCl$_3$ set at 77.0 ppm and Me$_4$Sn set at 0.00 ppm, respectively. CP-MAS ^{117}Sn spectra were recorded at 89.15 MHz on a Bruker Avance 250 spectrometer, equipped with a 4 or 7 mm MAS broadband probe. The chemical shift reference was set with (cyclo-C$_6$H$_{11}$)$_4$Sn (−97.35 ppm relative to (CH$_3$)$_4$Sn). The positive-ion and negative-ion electrospray ionization (ESI) mass spectra were measured using an Esquire 3000 ion trap analyzer (Bruker Daltonics, Bremen, Germany) in the range *m/z* 50–2000. The samples were dissolved in acetonitrile for positive-ion mode or in methanol for negative-ion mode measurements and analyzed by direct infusion at a flow rate of 5 μl/min. The selected precursor ions were further analyzed by MS/MS analyses under the following conditions: isolation width of *m/z* = 8 for ions containing one tin atom and *m/z* = 12 for ions containing


Fig. 1. Structure of the ligand framework. Abbreviations: L^{1}HK: R^1 = H; R^2 = H, L^{2}HK: R^1 = CH$_3$; R^2 = H, L^{3}HK: R^1 = CH$_3$; R^2 = CH$_3$.

more tin atoms, collision amplitude in the range 0.7–1.0 V depending on the precursor ion stability, an ion source temperature of 300 °C, a flow rate and pressure of nitrogen of 4 l/min and 10 psi, respectively. The compound stability tuning parameter was set to 100% in all cases, except for the positive-ion ESI-MS of **1**, **2** and **3** (20%). The subscripts "mono", "di", "tri" and "tetra" in the lists of observed ions mean monomeric, dimeric, trimeric and tetrameric molecules.

2.3. Synthesis of potassium 2-{[(E)-1-(2-oxyaryl)-alkylidene]amino}acetates

The potassium 2-{[(E)-1-(2-oxyaryl)alkylidene]-amino}acetates (L^1HK–L^3HK, see Fig. 1) were prepared as described in earlier reports [3,5,6].

2.4. Synthesis of diorganotin(IV) 2-{[(E)-1-(2-oxyaryl)-alkylidene]amino}acetates

The diorganotin(IV) complexes **1**–**5** were prepared by reacting equimolar quantities of the potassium salt of the appropriate ligand (LHK, Fig. 1) and the respective diorganotin dichlorides in anhydrous methanol, followed by proper work-up as described in our earlier report [5]. The ^1H and ^{13}C NMR data for the compounds **1**, **2** and **5** corresponded with those described elsewhere [5] while the data for **4** are given below. Compound **6** was prepared by reacting equimolar amounts of diphenyltin(IV) 2-{[(E)-1-(2-oxyphenyl)ethylidene]amino}-acetate (prepared by reacting potassium- 2-{[(E)-1-(2-hydroxyphenyl)ethylidene]amino}acetate and diphenyltin dichloride [3]) and 1,10-phenanthroline in anhydrous benzene. The steps involved in the work-up and purification of **6** are described below.

2.4.1. Synthesis of [Me₂Sn(2-OC₆H₄C(CH₃)=NCH₂-COO)(OH₂)]₂ (1)

Pale yellow crystals of compound **1**, m.p. 210–211 °C, were obtained from benzene after dissolution of the powdered sample [5]. Anal. Found: C, 40.30; H, 4.80; N, 3.92%. Calc. for $C_{24}H_{34}N_2O_8Sn_2$: C, 40.27; H, 4.78; N, 3.91%. Positive-ion MS: m/z 1365 [M_{tetra} + H]$^+$; m/z 721 [M_{di} + K]$^+$; m/z 705 [M_{di} + Na]$^+$, 100%; m/z 380 [M_{mono} + K]$^+$; m/z 364 [M_{mono} + Na]$^+$. MS/MS of m/z 1365: m/z 1024 [M_{tri} + H]$^+$; m/z 697. MS/MS of m/z 721: m/z 380 [M_{mono} + K]$^+$. MS/MS of m/z 705: m/z 364 [M_{mono} + Na]$^+$. MS/MS of m/z 364: m/z 320 [M_{mono} + Na − CO_2]$^+$; m/z 299. Negative-ion MS: m/z 340 [M_{mono} − H]$^-$, 100%. MS/MS of m/z 340: m/z 312 [M_{mono} − H − CO]$^-$; m/z 296 [M_{mono} − H − CO_2]$^-$; m/z 205 [O(CH₃)₂SnONa]$^-$; m/z 146 [M_{mono} − (CH₃)₂ SnOCOH]$^-$.

2.4.2. Synthesis of [ⁿBu₂Sn(2-OC₆H₄C(CH₃)=NCH₂-COO)(OH₂)]₂ (2)

Colourless crystals of compound **2**, m.p. 77–78 °C, were obtained from a mixture of chloroform and hexane (v/v 1:4) after dissolution of the pale yellow powdered sample [5]. Anal. Found: 48.95; H, 6.60; N, 3.20%. Calc. for $C_{36}H_{58}N_2O_8Sn_2$: C, 48.91; H, 6.61; N, 3.17%. Positive-ion MS: m/z 1314 [M_{tri} + K]$^+$; m/z 1298 [M_{tri} + Na]$^+$, 100%; m/z 889 [M_{di} + K]$^+$; m/z 873 [M_{di} + Na]$^+$; m/z 464 [M_{mono} + K]$^+$; m/z 448 [M_{mono} + Na]$^+$; m/z 426 [M_{mono} + H]$^+$. MS/MS of m/z 1314: m/z 889 [M_{di} + K]$^+$; m/z 464 [M_{mono} + K]$^+$. MS/MS of m/z 1298: m/z 873 [M_{di} + Na]$^+$; m/z 448 [M_{mono} + Na]$^+$. MS/MS of m/z 889: m/z 464 [M_{mono} + K]$^+$. MS/MS of m/z 873: m/z 448 [M_{mono} + Na]$^+$. MS/MS of m/z 448: m/z 404 [M_{mono} + Na − CO_2]$^+$; m/z 334 [M_{mono} + Na − butene − butane]$^+$. Negative-ion MS: m/z 424 [M_{mono} − H]$^-$, 100%. MS/MS of m/z 424: m/z 310 [M_{mono} − H − butene − butane]$^-$; m/z 146 [M_{mono} − H − SnBu₂ − CO_2]$^-$.

2.4.3. Synthesis of [ⁿBu₂Sn(2-OC₆H₄C(H)=NCH₂-COO)]₃·0.5C₃H₆O (3)

During the attempted preparation of [ⁿBu₂Sn-L¹(OH₂)] [5], crystallization from acetone afforded **3** as pale yellow crystals in 68% yield, m.p. 124–125 °C. Anal. Found: C, 50.09; H, 6.20; N, 3.30%. Calc. for $C_{52.5}H_{78}N_3O_{9.5}Sn_3$: C, 50.08; H, 6.24; N, 3.33%. IR (cm^{-1}): 1620 v(OCO)$_{asym}$, 1585 v(C=N), 1390 v(OCO)$_{sym}$, 1250 v(Ph(C–O)). ^1H NMR(CDCl₃)[1]: Ligand skeleton: 8.40 (s, 1H, H-3′), 7.43 (t, 1H, H-9), 7.18 (d, 1H, H-7), 6.79 (d, 1H, H-6), 6.74 (t, 2H, H-8), 4.34 (s, 3H, H-2); Sn–Bu skeleton: 1.64 (m, 4H, H-3*), 1.58 (m, 4H, H-1*), 1.38 (m, 4H, H-2*), 0.87 (t, 6H, H-4*) ppm. ^{13}C NMR (CDCl₃)[1]: Ligand skeleton: 172.9 (C-1), 171.4 (C-3), 169.5 (C-5), 138.0 (C-7), 135.6 (C-9), 122.7 (C-6), 117.3 (C-4), 117.2 (C-8), 57.7 (C-2); Sn–Bu skeleton: 26.8 (C-2*), 26.7 (C-1*), 22.6 (C-3*), 13.7 (C-4*) ppm. Positive-ion MS: m/z 1256 [M_{tri} + Na]$^+$; m/z 861 [M_{di} + K]$^+$; m/z 845 [M_{di} + Na]$^+$,100%; m/z 450 [M_{mono} + K]$^+$; m/z 434 [M_{mono} + Na]$^+$. MS/MS of m/z 1256: m/z 845 [M_{di} + Na]$^+$; m/z 434 [M_{mono} + Na]$^+$. MS/MS of m/z 861: m/z 450 [M_{mono} + K]$^+$. MS/MS of m/z 845: m/z 434 [M_{mono} + Na]$^+$. MS/MS of m/z 434: m/z 390 [M_{mono} + Na − CO_2]$^+$; m/z 320 [M_{mono} + Na − butene − butane]$^+$. Negative-ion MS: m/z 468 [M_{mono} − H + butane]$^-$; m/z 442 [M_{mono} − H + CH₃OH]$^-$; m/z 410 [M_{mono} − H]$^-$, 100%; m/z 358 [M − H − 2*butane + 2*CH₃OH]$^-$; m/z 239 [(CH₃O)₂ SnBu]$^-$; m/z 213 [(CH₃O)₃Sn]$^-$. MS/MS of m/z 468: m/z 354 [M_{mono} − H − butene]$^-$; m/z 310 [M_{mono} − H − butene − CO_2]$^-$. MS/MS of m/z 410: m/z 296 [M_{mono} − H − butene − butane]$^-$; m/z 132 [M_{mono} − H − SnBu₂ − CO_2]$^-$. MS/MS of m/z 358: m/z 326

$[M_{mono} - H - 2*butane + CH_3OH]^-$; m/z 282 $[M_{mono} - H - 2*butane + CH_3OH - CO_2]^-$; m/z 250 $[M_{mono} - H - 2*butane - CO_2]^-$; m/z 176 $[M_{mono} - H - SnBu_2]^-$; m/z 132 $[M_{mono} - H - SnBu_2 - CO_2]^-$.

2.4.4. Synthesis of $[^nBu_2Sn(2-OC_6H_3(CH_3-3)-C(CH_3)=NCH_2COO)]_3 \cdot 0.5C_6H_6$ (4)

A procedure similar to that used to prepare compounds **2** and **3** was followed [5]. A methanol solution (5 ml) containing $^nBu_2SnCl_2$ (0.50 g, 1.64 mmol) was added drop-wise to previously dissolved L^3HK (0.40 g, 1.63 mmol) in 50 ml methanol under stirring conditions. The reaction mixture was refluxed for 5 h, the volatiles were removed and the residue was washed with petroleum ether (60–80 °C). The yellow-coloured solid mass was dissolved in benzene (30 ml) and filtered. The filtrate was reduced to one fourth of its initial solvent volume, cooled to r.t. and 20 ml of hexane was added. The clear solution was allowed to evaporate at r.t., which afforded yellow crystals of **4** in 60% (0.43 g) yield, mp 99–100 °C. Anal. Found: C, 53.20; H, 6.80; N, 3.15%. Calc. for $C_{60}H_{90}N_3O_9Sn_3$: C, 53.25; H, 6.70; N, 3.10%. IR (cm^{-1}): 1600–1585 $v(OCO)_{asym} + v(C=N)$, 1242 $v(Ph-(C-O))$. ^1H NMR $(CDCl_3)^1$: Ligand skeleton: 7.32 (t, 1H, H-9), 7.26 (d, 1H, H-7), 6.66 (t, 1H, H-8), 4.23 (s, 2H, H-2), 2.63 (s, 3H, H-3′), 2.16 (s, 3H, H-6′); Sn–Bu skeleton: 1.59 (m, 4H, H-3*), 1.43 (m, 4H, H-1*), 1.32 (m, 4H, H-2*), 0.86 (t, 6H, H-4*) ppm. ^{13}C NMR $(CDCl_3)^1$: Ligand skeleton: 181.5 (C-1), 170.5 (C-3), 164.8 (C-5), 136.0 (C-7), 131.8 (C-9), 127.9 (C-4), 120.2 (C-6), 116.9 (C-8), 53.5 (C-2), 22.8 (C-3′), 16.4 (C-6′); Sn–Bu skeleton: 26.9 (C-2*), 26.6 (C-1*), 20.9 (C-3*), 13.4 (C-4*) ppm. Positive-ion MS: m/z 1356 $[M_{tri} + K]^+$; m/z 1340 $[M_{tri} + Na]^+$; m/z 917 $[M_{di} + K]^+$; m/z 901 $[M_{di} + Na]^+$, 100%; m/z 879 $[M_{di} + H]^+$; m/z 478 $[M_{mono} + K]^+$; m/z 462 $[M_{mono} + Na]^+$; m/z 440 $[M_{mono} + H]^+$. MS/MS of m/z 1340: m/z 901 $[M_{di} + Na]^+$. MS/MS of m/z 917: m/z 478 $[M_{mono} + K]^+$. MS/MS of m/z 901: m/z 462 $[M_{mono} + Na]^+$. MS/MS of m/z 462: m/z 348 $[M_{mono} + Na-butene-butane]^+$. Negative-ion MS: m/z 438 $[M_{mono} - H]^-$, 100%; m/z 353 $[Bu_2SnCl_2OCH_3+H_2O]^-$. MS/MS of m/z 438: m/z 324 $[M_{mono} - H - butene - butane]^-$; m/z 160 $[M_{mono} - H - SnBu_2 - CO_2]^-$. MS/MS of m/z 353: m/z 339; m/z 323 $[Bu_2SnCl_2OCH_3 + H_2O - HCOH]^-$; m/z 265 $[Bu_2SnCl_2OCH_3 - Cl_2]^-$; m/z 209 $[Bu_2SnCl_2-OCH_3 - Cl_2 - butene]^-$.

2.4.5. Synthesis of $[Ph_2Sn(2-OC_6H_3(CH_3-3)-C(CH_3)=NCH_2COO)] \cdot 0.5C_6H_6$ (5)

Yellow crystals of compound **5**, m.p. 189–191 °C, were obtained from benzene upon dissolution of $Ph_2Sn(2-OC_6H_3(CH_3-3)C(CH_3)=NCH_2COO)$ (m.p.

170–172 °C) [5]. Anal. Found: C, 60.45; H, 4.75; N, 2.70%. Calc. for $C_{26}H_{24}NO_3Sn$: C, 60.39; H, 4.67; N, 2.70%. Positive-ion MS: m/z 1476 $[M_{tri} + K]^+$; m/z 1460 $[M_{tri} + Na]^+$; m/z 997 $[M_{di} + K]^+$; m/z 981 $[M_{di} + Na]^+$, 100%; m/z 518 $[M+K]^+$; m/z 502 $[M_{mono} + Na]^+$; m/z 480 $[M_{mono} + H]^+$. MS/MS of m/z 1476: m/z 997 $[2*M_{mono} + K]^+$; m/z 518 $[M_{mono} + K]^+$. MS/MS of m/z 1460: m/z 981 $[M_{di} + Na]^+$; m/z 502 $[M_{mono} + Na]^+$. MS/MS of m/z 997: m/z 518 $[M_{mono} + K]^+$. MS/MS of m/z 982: m/z 502 $[M_{mono} + Na]^+$. MS/MS of m/z 480: m/z 420 $[M_{mono} - HAC + H]^+$. Negative-ion MS: m/z 478 $[M_{mono} - H]^-$, 100%; m/z 393 $[Ph_2SnCl_2OCH_3+ H_2O]^-$. MS/MS of m/z 478: m/z 434 $[M_{mono} - H - CO_2]^-$; m/z 356 $[M_{mono} - H - CO_2 - benzene]^-$; m/z 329; m/z 274 $[SnPh_2 - H]^{--}$; m/z 160 $[M_{mono} - H - CO_2 - SnPh_2]^-$. MS/MS of m/z 393: m/z 363 $[Ph_2SnCl_2-OCH_3 + H_2O - HCOH]^-$; m/z 305 $[Ph_2Sn-Cl_2OCH_3 - Cl_2]^-$; m/z 285 $[PhSnCl_2 + H_2O]^-$; m/z 275 $[Ph_2SnCl_2OCH_3 - HCOH - Cl_2]^-$.

2.4.6. Synthesis of $[Ph_2Sn(2-OC_6H_4C(CH_3)=NCH_2-COO)(Phen)]$ (6)

Diphenyltin(IV) 2-{[(E)-1-(2-oxyphenyl)ethylidene]-amino}acetate was prepared (yellow block-shaped crystals, m.p. 221–222 °C) [3] and characterized by microanalysis, IR (KBr: 1682 cm^{-1} $v(OCO)_{asym}$), ^1H; ^{13}C; and ^{119}Sn (CDCl₃ solution: −351.7 ppm) NMR, and ^{119}Sn Mössbauer ($\delta = 1.15$, $\Delta = 2.88$, $\Gamma_1\pm$ and $\Gamma_2 \pm = 0.89$ and 0.98 mm s^{-1}, Ph–Sn–Ph = 128°) spectroscopic techniques. This sample was used for the subsequent synthesis. A warm benzene solution of 1,10-phenanthroline (5 ml, 0.19 g, 0.96 mmol) was added drop-wise to a hot stirred benzene solution of diphenyltin(IV) 2-{[(E)-1-(2-oxyphenyl)ethylidene]-amino}acetate (20 ml, 0.45 g, 0.96 mmol). Rapid formation of a white-coloured precipitate was observed. The reaction mixture was then refluxed for an additional 30 min and was filtered while hot. The residue was collected and dried in vacuo. The dried residue was dissolved in anhydrous benzene/chloroform mixture (1:2, 15 ml) and filtered off to remove any suspended particles. The filtrate was kept for slow evaporation at room temperature which furnished colourless crystals of **6** (0.27 g, 55%); m.p. 233–234 °C. Anal. Found: C, 63.45; H, 4.25; N, 6.50%. Calc. for $C_{34}H_{27}N_3O_3Sn$: C, 63.39; H, 4.22; N, 6.52%. IR (cm^{-1}): 1660 $v (OCO)_{asym}$, 1600 $v(C=N)$, 1439 $v(OCO)_{sym}$, 1235 $v(Ph(C-O))$. ^1H NMR $(CDCl_3)^1$: Ligand skeleton: 7.40 (d, 1H, H-9), 7.19 (t, 1H, H-7), 7.18 (d, 1H, H-6), 6.73 (t, 1H, H-8), 4.26 (s, 2H, H-2), 2.58 (s, 3H, H-3′); Sn–Ph skeleton: 7.90 (m, 4H, H-2*), 7.38 (m, 6H, H-3* and H-4*); Phen: 9.41 (d, 2H, H-2 and H-9), 8.25 (d, 2H, H-4 and H-7), 7.68 (dd, 4H, H-3; H-8; H-5 and H-6) ppm. ^{13}C NMR

(CDCl$_3$)[1]: Ligand skeleton: 181.1 (C-1), 171.0 (C-3), 166.8 (C-5), 136.7 (C-7), 130.9 (C-9), 124.0 (C-6), 121.0 (C-4), 117.8 (C-8), 53.9 (C-2), 22.8 (C-3′); Sn–Ph skeleton: 139.5 (C-1*), 136.4 (C-2*), 130.5 (C-4*), 128.9 (C-3*); Phen: 150.7 (C-2 and C-9), 145.9 (C-10a and C-10b), 136.2 (C-4 and C-7), 128.5 (C-4a and C-4b), 126.7 (C-5 and C-6), 123.4 (C-3 and C-8), ppm. Positive-ion MS: m/z 684 [M + K]$^+$; m/z 668 [M + Na]$^+$; m/z 646 [M + H]$^+$; m/z 399 [2*Phen+K]$^+$; m/z 383 [2*Phen + Na]$^+$; m/z 219 [Phen + K]$^+$; m/z 203 [Phen + Na]$^+$, 100%; m/z 181 [Phen + H]$^+$. MS/MS of m/z 684: m/z 504 [M + K-Phen]$^+$; m/z 219 [Phen + K]$^+$. MS/MS of m/z 668: m/z 488 [M + Na-Phen]$^+$; m/z 203 [Phen + Na]$^+$. MS/MS of m/z 646: m/z 181 [Phen + H]$^+$. MS/MS of m/z 399: m/z 219 [Phen + K]$^+$. MS/MS of m/z 383: m/z 203 [Phen + Na]$^+$. Negative-ion MS: m/z 464 [M – H – Phen]$^-$, 100%; m/z 397 [Ph$_2$SnCl$_3$ + H$_2$O]$^-$. MS/MS of m/z 464: m/z 420 [M – H – Phen – CO$_2$]$^-$; m/z 342 [M – H – Phen – CO$_2$ – benzene]$^-$; m/z 315; m/z 274 [SnPh$_2$ – H]$^-$; m/z 146 [M – H – Phen – CO$_2$ – SnPh$_2$]$^-$. MS/MS of m/z 397: m/z 309 [Ph$_2$SnCl$_3$ – Cl$_2$]$^-$.

2.5. X-ray crystallography

Crystals of compounds **1**–**6** suitable for an X-ray crystal-structure determination were obtained from benzene (**1**, **5**), hexane/chloroform (**2**), acetone (**3**), hexane/benzene (**4**) or benzene/chloroform (**6**). All measurements were made on a Nonius KappaCCD diffractometer [9] with graphite-monochromated Mo Kα radiation ($\lambda = 0.71073$ Å) and an Oxford Cryosystems Cryostream 700 cooler. Data reduction was performed with HKL Denzo and Scalepack [10]. The intensities were corrected for *Lorentz* and polarization effects, and empirical absorption corrections based on the multiscan method [11] were applied. Equivalent reflections were merged, other than the *Friedel* pairs for **2** and **3**. The data collection and refinement parameters are given in Table 1, and views of the molecules are shown in

---

[1] For the ^{1}H and ^{13}C NMR assignments, refer to Fig. 1 for the numbering scheme of the ligand skeleton, while for the Sn–R and Phen skeletons, the numbering is as shown below:

Figs. 2–8. The structures were solved by direct methods using SHELXS97 [12] for **1** and **3**, and SIR92 [13] for **2**, and **4**–**6**. For each structure, the non-hydrogen atoms were refined anistropically while employing similarity restraints on chemically equivalent geometric and atomic displacement parameters, when necessary, to refine any disordered moieties in the structures, as described below.

In **3**, there are two symmetry-independent molecules of the trinuclear Sn complex (molecules A and B) plus two sites for solvent molecules in the asymmetric unit. No additional symmetry was evident [14]. All atoms of both butyl substituents of one Sn atom and one butyl substituent of another Sn atom in molecule A, as well as both butyl substituents of one Sn atom in molecule B are disordered over two conformations. The two symmetry-independent sites for solvent molecules appear to be about 50% occupied by highly disordered acetone molecules. The acetone molecules could not be modeled adequately, so the SQUEEZE routine of the program PLATON [14,15] was employed in order to obviate having to include solvent molecules in the model. The program estimates that there are four cavities of 229 Å^3 per unit cell with approximately 36 e per cavity. In **4a**, the asymmetric unit contains one molecule of the trinuclear Sn-complex plus half a molecule of benzene, with the benzene molecule sitting about a crystallographic C_2-axis. One butyl group at each Sn atom is disordered over two equally occupied conformations. Compound **4b** has the same composition and disorder, except that the benzene molecule sits about a crystallographic inversion centre. In **5**, the asymmetric unit contains one molecule of the trinuclear Sn-complex plus half a molecule of benzene, with the benzene molecule sitting about a crystallographic inversion centre.

The H atoms of the water ligands of **1** and **2** were placed in the positions indicated by a difference *Fourier* map and their positions were allowed to refine together with individual isotropic displacement parameters. All other H atoms in all structures were placed in geometrically calculated positions and refined using a riding model where each H atom was assigned a fixed isotropic displacement parameter with a value equal to $1.2U_{eq}$ of its parent C atom ($1.5U_{eq}$ for the methyl groups). The refinement of each structure was carried out on F^2 using full-matrix least-squares procedures, which minimized the function $\sum w(F_o^2 - F_c^2)^2$. Corrections for secondary extinction were applied for **1**, **4b**, **5** and **6**. Compounds **2** and **3** crystallize in non-centrosymmetric space groups and refinement of the absolute structure parameter [16] yielded values of 0.08(2) and 0.30(2), respectively. The former value indicates that the correct absolute structure of **2** has been defined by the model, while the latter value suggests that the crystals of **3** are inversion twins. All calculations were performed using the SHELXL97 [17] program.
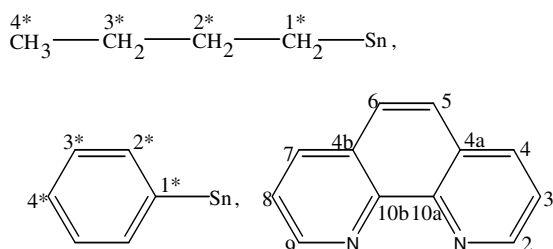
Table 1
Crystallographic data for compounds **1–6**

	1	**2**	**3**	**4a**	**4b**	**5**	**6**
Empirical formula	$C_{24}H_{34}N_2O_8Sn_2$	$C_{36}H_{58}N_2O_8Sn_2$	$C_{51}H_{75}N_3O_9Sn_3 \cdot 0.5$ (C_3H_6O)	$C_{57}H_{87}N_3O_9Sn_3 \cdot 0.5$ (C_6H_6)	$C_{57}H_{87}N_3O_9Sn_3 \cdot 0.5(C_6H_6)$	$C_{23}H_{21}NO_3Sn \cdot 0.5$ (C_6H_6)	$C_{34}H_{27}N_3O_3Sn$
Formula weight	715.74	884.06	1259.00	1353.18	1353.18	517.08	644.20
Crystal size (mm)	$0.07 \times 0.25 \times 0.30$	$0.12 \times 0.25 \times 0.30$	$0.20 \times 0.27 \times 0.30$	$0.15 \times 0.22 \times 0.25$	$0.15 \times 0.17 \times 0.17$	$0.12 \times 0.25 \times 0.25$	$0.12 \times 0.20 \times 0.20$
Crystal shape	Tablet	Prism	Prism	Prism	Prism	Prism	Prism
Temperature (K)	160(1)	160(1)	160(1)	160(1)	273(1)	160(1)	160(1)
Crystal system	Triclinic	Orthorhombic	Monoclinic	Monoclinic	Monoclinic	Monoclinic	Monoclinic
Space group	$P\bar{1}$	$P2_12_12_1$	Cc	$C2/c$	$P2_1/c$	$P2_1/n$	$C2/c$
a (Å)	7.8583(2)	9.5934(1)	31.7625(5)	24.4410(7)	19.0387(2)	14.5116(2)	36.9133(5)
b (Å)	9.4734(2)	16.9468(2)	16.5633(3)	13.3422(3)	13.5390(2)	8.9689(1)	10.1754(1)
c (Å)	9.9915(2)	23.8904(3)	24.3798(4)	39.153(1)	26.4835(3)	17.8300(3)	15.8335(2)
α (°)	105.1678(8)	90	90	90	90	90	90
β (°)	94.2532(9)	90	115.7833(8)	100.3497(8)	110.2506(6)	107.3972(5)	113.4519(6)
γ (°)	106.2070(9)	90	90	90	90	90	90
V (Å^3)	680.62(3)	3884.04(8)	11549.1(3)	12559.9(6)	6404.6(1)	2214.47(5)	5455.9(1)
Z	1	4	8	8	4	4	8
D_x (g cm^{-3})	1.746	1.512	1.448	1.431	1.403	1.551	1.568
μ (mm^{-1})	1.881	1.334	1.339	1.236	1.212	1.180	0.978
Transmission factors (min, max)	0.694, 0.884	0.682, 0.838	0.573, 0.755	0.595, 0.836	0.710, 0.839	0.767, 0.900	0.791, 0.894
$2\theta_{max}$ (°)	60	60	60	50	50	55	60
Reflections measured	17,844	51,464	85,468	59,522	109,441	52,404	69,321
Independent reflections; R_{int}	3968; 0.065	11,365; 0.054	32,183; 0.072	10,655; 0.089	11,307; 0.088	5074; 0.067	7990; 0.067
Reflections with $I > 2\sigma(I)$	3686	9812	25,878	7939	6605	4387	6131
Number of parameters	175	455	1375	803	794	283	372
Number of restraints	0	0	974	444	398	0	0
R (F) ($I > 2\sigma(I)$ reflns)	0.028	0.031	0.048	0.068	0.054	0.031	0.037
$wR(F^2)$ (all data)	0.072	0.073	0.116	0.166	0.147	0.080	0.089
GOF(F^2)	1.07	1.08	1.04	1.18	1.03	1.08	1.08
max, min $\Delta\rho$ (e/Å^3)	1.60, -1.53	1.79, -0.86	0.79, -1.13	1.16, -1.02	0.57, -0.83	1.04, -1.16	1.67, -1.18

3. Results and discussion

3.1. Synthetic aspects

Treatment of various diorganotin(IV)dichlorides with potassium 2-{[(E)-1-(2-hydroxyaryl)alkylidene]-amino}acetate yielded, after suitable work-up and recrystallization, compounds **1–5**. The basic physical characteristics of compounds **1**, **2** and **5** were found to be identical with those of the [R₂SnL(OH₂)] species reported earlier [5], while compounds **3** and **4** are the corresponding species minus the water ligand. Finally, the ability of diphenyltin(IV) 2-{[(E)-1-(2-oxyphenyl)ethylidene]amino}acetate to undergo additional coordination was studied by treating it with one equivalent of 1,10-phenanthroline, which yielded the adduct **6** in moderate yield. Compounds **1–6** are quite stable in air and can be recrystallized successfully from suitable organic solvents.

3.2. Crystal structures

The molecular structures of compounds **1–6** are shown in Figs. 2–8 (see Scheme 1 for line diagrams), while selected geometric parameters are collected in Tables 2–5. The molecule of **1** consists of centrosymmetric dimers of the basic $Me_2SnL^2(OH_2)$ moiety (Fig. 2), where the two Sn atoms are linked by two asymmetric Sn–O···Sn bridges involving the carboxylic acid O atom of the aminoacetate ligand and a long Sn···O(1)^i (symmetry operation i = − x, −y, −z) distance of 3.174(2) Å. As a consequence of atom O(1) bridging

two Sn atoms, the formal Sn–O(1) bond is longer than the corresponding bond in complexes **5** and **6** (Tables 4 and 5). In essence, **1** possesses a skeleton with a four-membered Sn_2O_2 ring. The long Sn···O contact is much shorter than the sum of the van der Waals radii of these atoms (3.78 Å), so the dimeric unit is the formal molecular entity that is present. Including the long contact, the coordination geometry about the Sn atom is a distorted pentagonal bipyramid, where two methyl groups adopt axial positions and the equatorial positions are occupied by the phenoxide O atom, one carboxylate O atom and the imino N atom of the tridentate aminoacetate ligand, one water ligand and the long Sn···O contact from the second $Me_2SnL^2(OH_2)$ moiety. If the long contact is ignored, the coordination geometry can be considered as a heavily distorted octahedron with one very open face, as shown by the O(1)–Sn–O(4) and C(10)–Sn–C(11) angles. However, such an open face cannot be attributed entirely to the restricted bite angles of the tridentate ligand, thereby confirming the significance of the Sn···O(1)^i interaction. The divinyltin analogue [3] was found to possess essentially the same structure with the same space group and similar unit cell dimensions. An even longer Sn···O contact of 3.319(4) Å was noted there, but the complex was not described as a formal dimer. The tridentate ligand in **1** is not planar, as noted previously [3], being bent most significantly about the C(3)···O(3)-axis, but the atoms N(1), O(1), O(3), O(4) and Sn are all coplanar.

A view of the unit cell contents for **1** is shown in Fig. 3. The water ligand acts as a donor for two hydrogen bonds. One is an intramolecular interaction with the
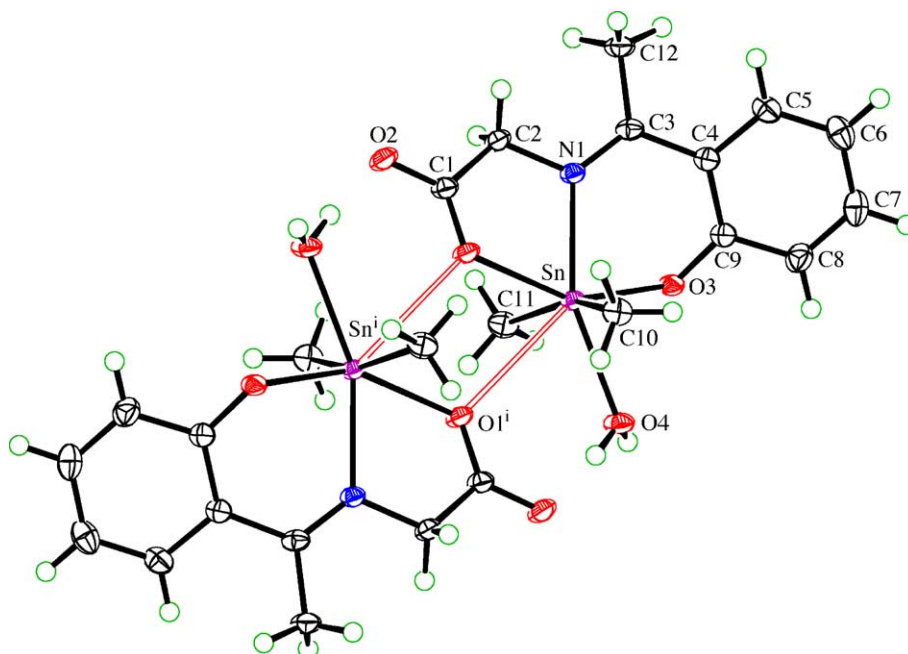

Fig. 2. The structure of the dimeric unit of **1** with the atom-labelling scheme (50% probability ellipsoids; symmetry operation i = − x, −y, −z).
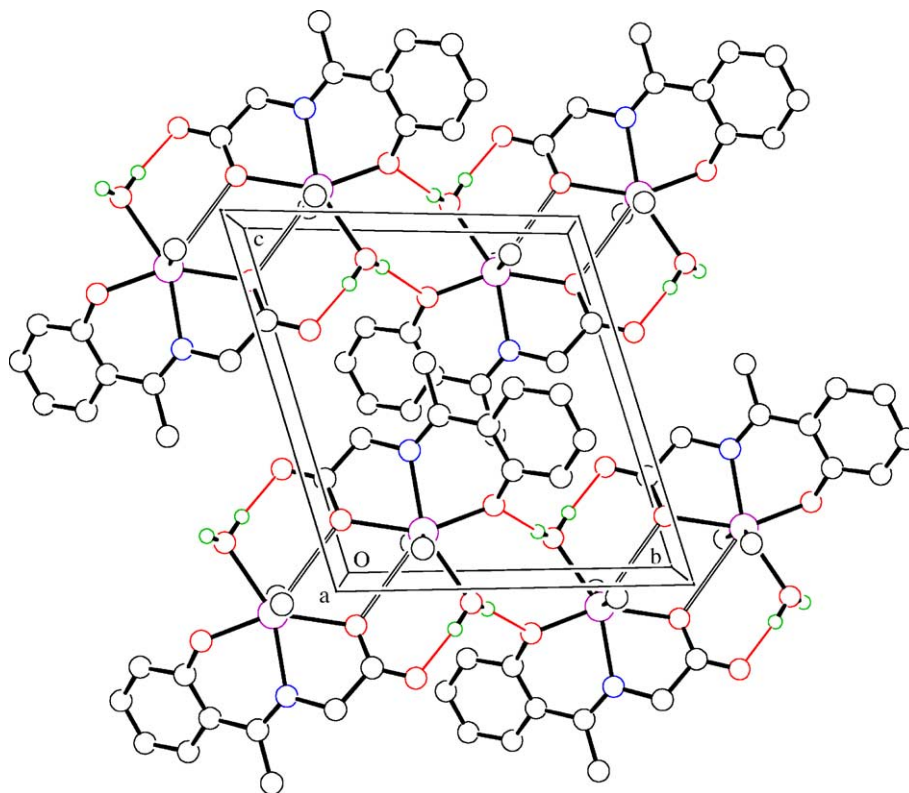
Fig. 3. The molecular packing of **1** viewed down the *a*-axis showing the dimeric units linked into columns along the [0 1 0] direction by hydrogen bonds (thin lines). Most H atoms omitted for clarity.
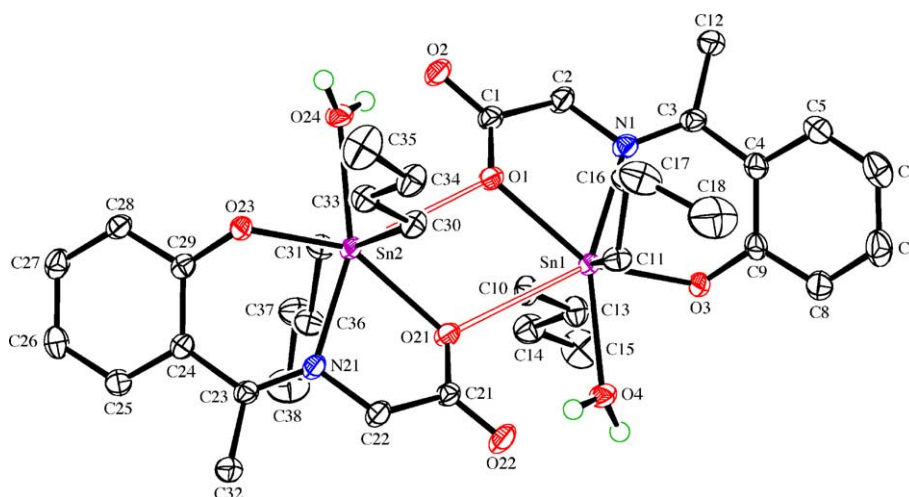

Fig. 4. The structure of the dimeric unit of **2** with the atom-labelling scheme (50% probability ellipsoids; H atoms omitted for clarity).

carboxylate carbonyl O(4)[i] atom of the second moiety in the dimeric molecule. This interaction forms a six-membered loop which has a graph set motif [18] of S(6). The symmetry of the dimeric molecule results in two of these motifs per molecule, which can be combined and represented by a binary graph set motif of $R_2^2(12)$. The second interaction is intermolecular and involves the phenoxide O(3)[ii] atom (symmetry operation ii = −*x*, 1 − *y*, −*z*) of an adjacent dimeric molecule, which is related to the original molecule by a centre of inversion. As a result, the second molecule has an identical interaction with the original molecule and these two interactions combine to give a closed loop with a graph set motif of $R_2^2(8)$. Because of the symmetry within the dimeric molecule, these interactions are repeated on the opposite side of the dimer with the net result being the generation of doubly bridged hydrogen-bonded columns which run parallel to the crystallographic [0 1 0] direction.
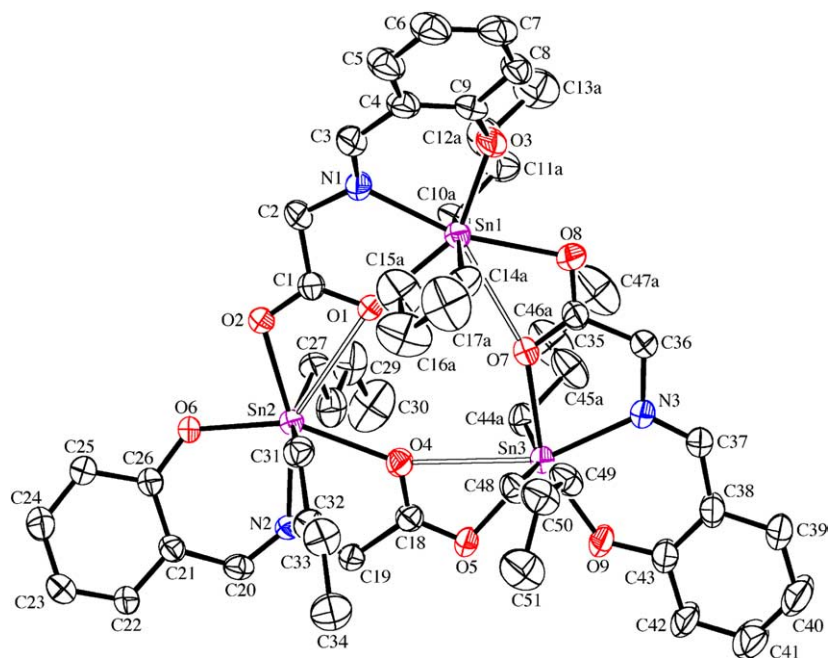
Fig. 5. The molecular structure of the major disordered conformation of one of the two symmetry-independent molecules of **3** with the atom-labelling scheme (50% probability ellipsoids; H atoms omitted for clarity).
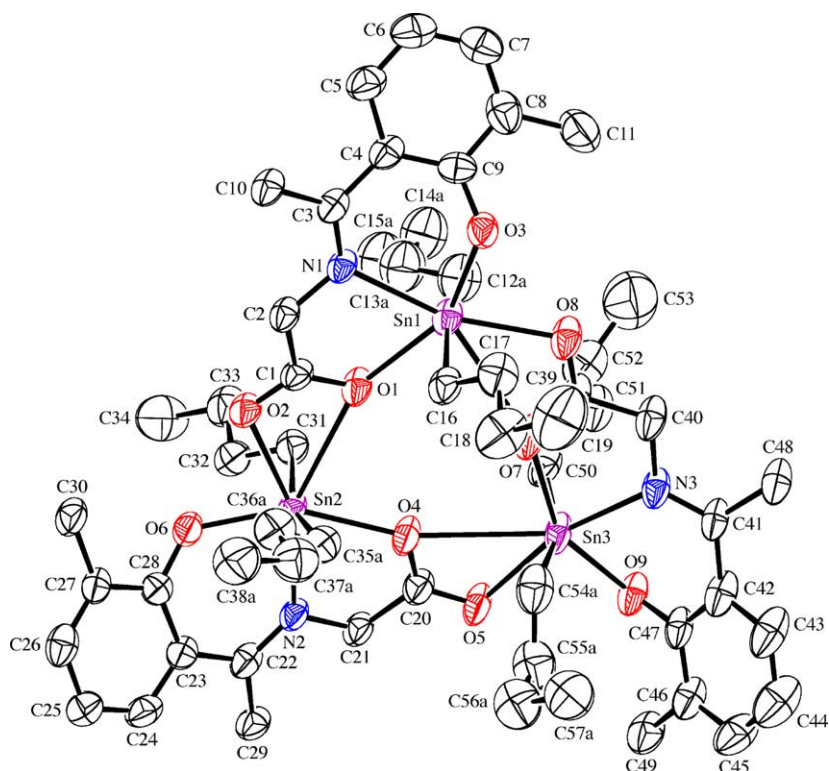
Fig. 6. The molecular structure of the major disordered conformation of **4a** with the atom-labelling scheme (50% probability ellipsoids; H atoms and solvent molecules omitted for clarity).

The crystal structure of compound **2** exhibits the same dimeric $[R_2SnL(OH_2)]_2$ structural motif and Sn atom coordination geometry as compound **1**. The only significant difference between the structures is that the dimeric unit in **2** does not sit about a crystallographic centre of inversion and therefore only has approximate inversion symmetry (Fig. 4). The chemically equivalent, but crystallographically independent asymmetric
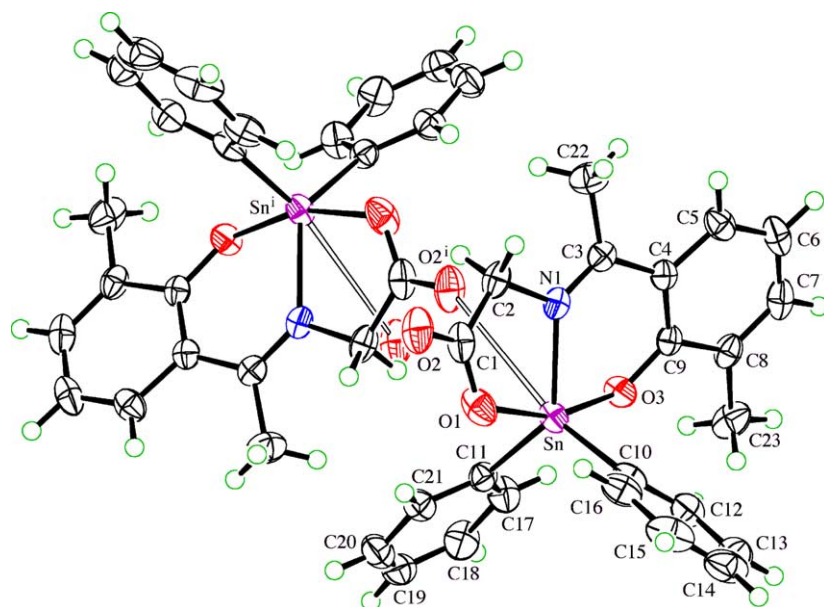
Fig. 7. The structure of **5** with the atom-labelling scheme and showing two units of the *cis*-bridged Ph$_2$SnL chain (50% probability ellipsoids; symmetry operation i = 0.5 − *x*, 0.5 + *y*, 1.5 − *z*). Solvent molecules omitted.
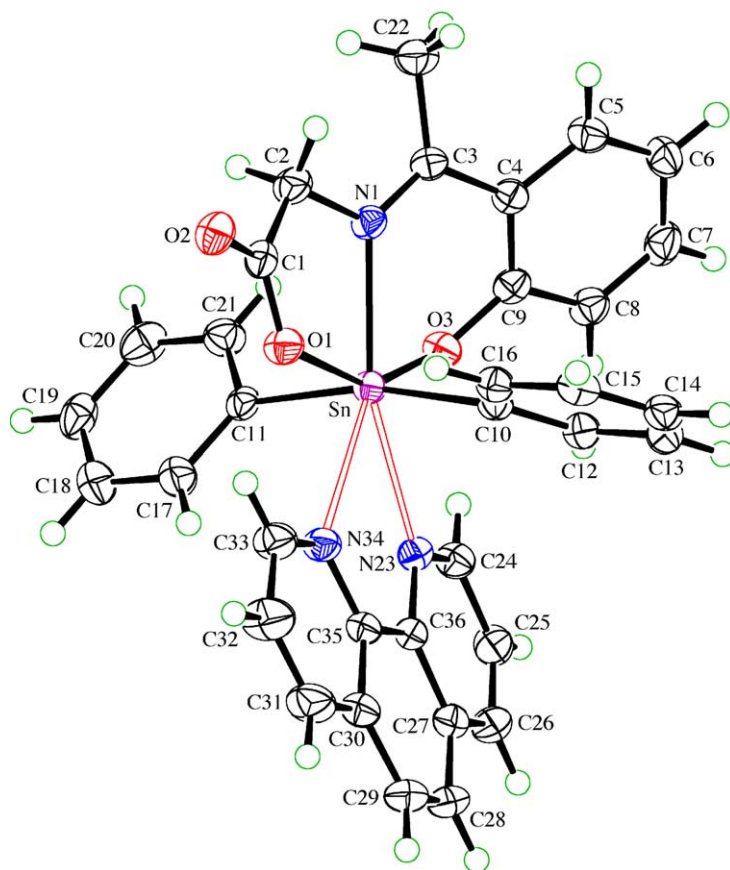
Fig. 8. The molecular structure of **6** with the atom-labelling scheme (50% probability ellipsoids).

Sn–O···Sn bridges in **2** have Sn···O distances of 3.079(2) and 3.086(3) Å and are about 0.09 Å shorter than the corresponding distance in **1**. All other geomet-

ric parameters are not significantly different to those of compound **1**. The pattern of hydrogen bonds in **2** is the same as that observed in **1**, although the doubly
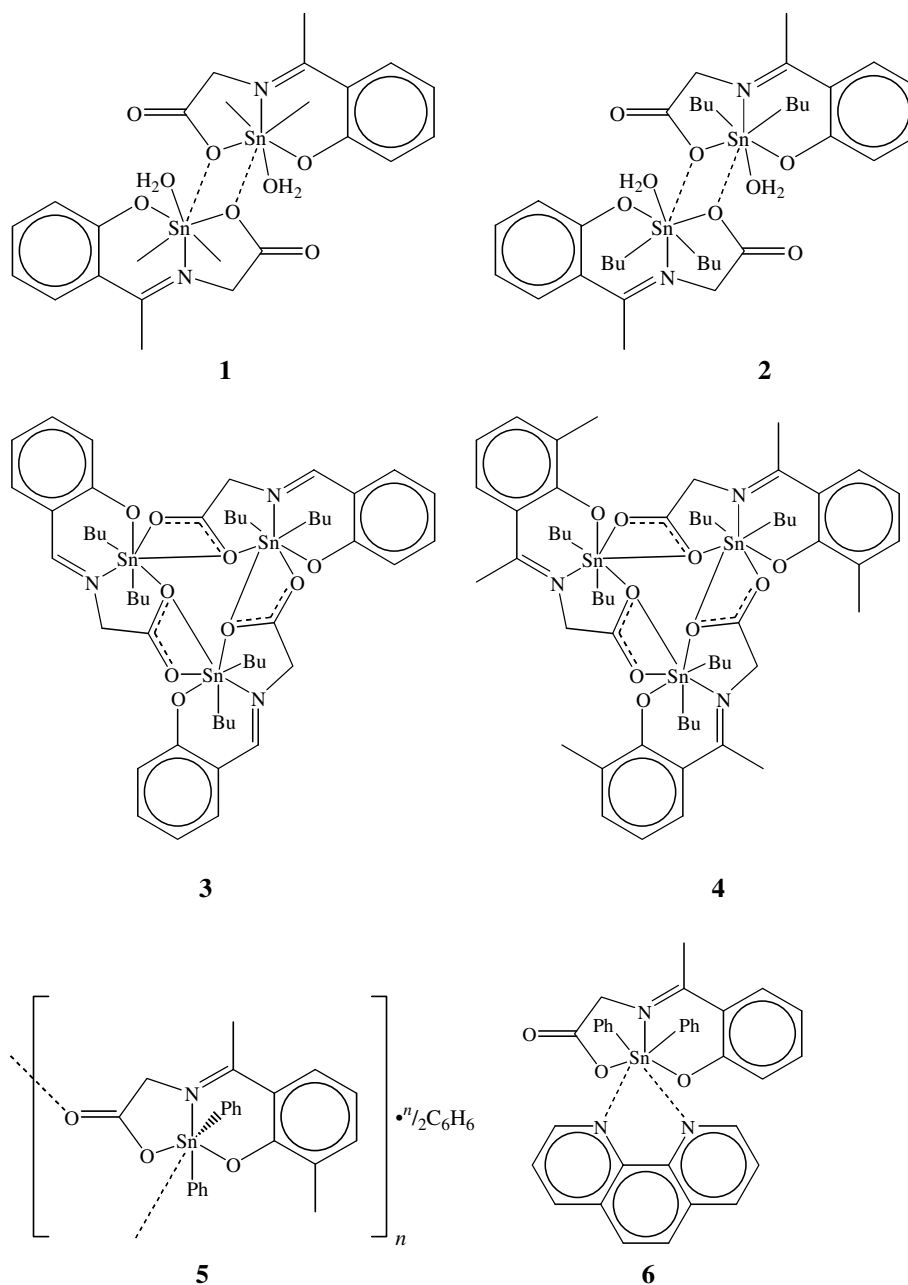
Scheme 1. Structures of the complexes **1**–**6**.

bridged hydrogen-bonded columns now run parallel to the crystallographic [1 0 0] direction.

Compound **3** is a cyclic trinuclear [^{n}Bu$_2$SnL^1]$_3$ complex, which crystallizes as its acetone hemisolvate with two formula units in the asymmetric unit (Fig. 5). Each Sn atom in the molecule is coordinated in the usual way by one tridentate aminoacetate ligand and, additionally, in a bidentate fashion by both the *exo*- and *endo*-carboxylate O atoms from an adjacent aminoacetate ligand to form an equatorial plane, while the two butyl groups occupy axial positions (Table 3). Thus, the coordination geometry about the Sn atom is a distorted pentagonal bipyramid. The *exo*-, or carboxylate carbonyl, O atom

in the aminoacetate ligand forms the strongest bridging link between one ^{n}Bu$_2$SnL^1 moiety and the next Sn atom in the cyclic complex (mean Sn–O(*exo*): 2.35 Å). However, the *endo*-, or carboxylic acid, O atom also coordinates weakly to this second Sn atom (mean Sn$\cdots$O(*endo*): 2.96 Å), as well as strongly to the Sn atom about which the ligand has a tridentate interaction (mean Sn–O(*endo*): 2.34 Å), thereby generating an asymmetric Sn–O$\cdots$Sn bridge similar to that found in complexes **1** and **2**. The core of the trinuclear complex is thus defined by a six-membered Sn$_3$O$_3$ ring. Some of the butyl groups are disordered (see Section 2), in good agreement with the distribution of several isotropic

Table 2
Selected bond lengths (Å) and angles (°) for compound **1**[a]

Sn–O(1)	2.305(2)	Sn···O(1)[i]	3.174(2)
Sn–O(3)	2.098(2)	O(1)–C(1)	1.273(3)
Sn–O(4)	2.359(2)	O(2)–C(1)	1.240(3)
Sn–N(1)	2.287(2)	O(3)–C(9)	1.332(3)
Sn–C(10)	2.106(2)	N(1)–C(2)	1.466(3)
Sn–C(11)	2.105(2)	N(1)–C(3)	1.299(3)
O(1)–Sn–O(3)	150.66(6)	Sn–O(3)–C(9)	123.4(1)
O(1)–Sn–N(1)	71.85(6)	Sn–N(1)–C(2)	112.9(1)
O(1)–Sn–C(10)	87.18(8)	Sn–N(1)–C(3)	128.3(2)
O(1)–Sn–C(11)	86.11(8)	C(2)–N(1)–C(3)	118.9(2)
O(3)–Sn–N(1)	78.84(6)	Sn–O(1)···Sn[i]	117.30(5)
O(3)–Sn–C(10)	99.93(8)	C(1)–O(1)···Sn[i]	121.5(1)
O(3)–Sn–C(11)	96.38(8)	O(1)–Sn···O(1)[i]	62.70(5)
N(1)–Sn–C(10)	101.61(8)	O(3)–Sn···O(1)[i]	146.52(5)
N(1)–Sn–C(11)	96.61(8)	N(1)–Sn···O(1)[i]	134.50(5)
C(10)–Sn–C(11)	157.5(1)	C(10)–Sn···O(1)[i]	78.71(7)
Sn–O(1)–C(1)	117.4(1)	C(11)–Sn···O(1)[i]	79.15(7)

[a] Symmetry operation i = −x, −y, −z.

Table 4
Selected bond lengths (Å) and angles (°) for compound **5**[a]

Sn–O(1)	2.116(2)	O(2)–C(1)	1.217(3)
Sn–O(3)	2.049(2)	O(3)–C(9)	1.323(3)
Sn–N(1)	2.151(2)	N(1)–C(2)	1.470(3)
Sn–C(10)	2.132(3)	N(1)–C(3)	1.303(3)
Sn–C(11)	2.120(2)	Sn–O(2)[i]	3.491(2)
O(1)–C(1)	1.296(3)	O(2)–C(1)	1.217(3)
O(1)–Sn–O(3)	161.21(8)	Sn–O(3)–C(9)	127.3(2)
O(1)–Sn–N(1)	77.25(7)	Sn–N(1)–C(2)	112.7(2)
O(1)–Sn–C(10)	94.79(8)	Sn–N(1)–C(3)	127.5(2)
O(1)–Sn–C(11)	94.91(9)	C(2)–N(1)–C(3)	119.7(2)
O(3)–Sn–N(1)	84.73(7)	O(1)–C(1)–O(2)	124.1(3)
O(3)–Sn–C(10)	92.21(8)	Sn–O(2)[i]–O(1)[i]	145.5(2)
O(3)–Sn–C(11)	97.61(8)	O(1)–Sn–O(2)[i]	86.21(7)
N(1)–Sn–C(10)	113.30(8)	O(3)–Sn–O(2)[i]	79.23(6)
N(1)–Sn–C(11)	130.05(8)	N(1)–Sn–O(2)[i]	55.85(6)
C(10)–Sn–C(11)	116.50(9)	C(10)–Sn–O(2)[i]	168.65(7)
Sn–O(1)–C(1)	118.9(2)	C(11)–Sn–O(2)[i]	74.60(7)

[a] Symmetry operation i = 0.5 − x, 0.5 + y, 1.5 − z.

chemical shifts, close to one another in numerical value (see Table 5), found in the solid-state [117]Sn NMR spectrum of **3**. While the aminoacetate ligands themselves are mostly non-planar, as in **1**, the overall form of the trinuclear molecule has the aminoacetate ligands and Sn atoms in one plane with the butyl ligands all roughly perpendicular thereto.

Compound **4** is a cyclic trinuclear [[n]Bu₂SnL³]₃ complex with a molecular structure similar to that of **3** and was found to crystallize in two polymorphic forms. Both forms are of the benzene hemisolvate with one formula unit in the asymmetric unit. In form **4a**, the benzene molecule sits about a crystallographic C_2-axis, while in form **4b**, the benzene molecule sits about a cen-

tre of inversion. The only difference between the structure of the trinuclear moiety in **3** and those in **4a** and **4b** is the presence of two additional methyl groups on the aminoacetate ligands of the latter compounds. Otherwise, the coordination geometry about each Sn atom in **4a** (Fig. 6) and **4b** is the same as in **3** and all geometric parameters are within or close to the ranges given for **3** in Table 3. Both polymorphs came from the same crystallization vial. Several weeks after the crystals were grown and isolated from their mother liquor, the structure of form **4a** was determined first and at −113 °C. In an attempt to repeat the data collection seven days later, several new crystals were selected from the vial, but did not survive cooling to −113 °C. The crystal integrity

Table 3
Selected bond lengths (Å) and angles (°) for compound **3**[a]

Sn(1)–O(1)	2.309(4)–2.359(4)	Sn(1)–O(8)	2.288(4)–2.408(4)
Sn(1)–O(3)	2.078(4)–2.113(4)	O(1)–C(1)	1.248(7)–1.263(7)
Sn(1)–N(1)	2.257(4)–2.291(5)	O(2)–C(1)	1.250(7)–1.261(7)
Sn(1)–C(10a)	2.111(5)–2.126(4)	O(3)–C(9)	1.294(7)–1.325(7)
Sn(1)–C(14a)	2.117(6)–2.139(6)	N(1)–C(2)	1.464(7)–1.482(7)
Sn(1)–O(7)	2.874(4)–3.044(4)	N(1)–C(3)	1.269(7)–1.295(7)
O(1)–Sn(1)–O(3)	150.3(1)–154.2(2)	O(8)–Sn(1)–N(1)	156.7(1)–166.3(1)
O(1)–Sn(1)–O(7)	75.0(1)–83.7(1)	O(8)–Sn(1)–C(10a)	81.9(3)–89(1)
O(1)–Sn(1)–O(8)	121.8(1)–132.0(1)	O(8)–Sn(1)–C(14a)	83.9(2)–87.4(9)
O(1)–Sn(1)–N(1)	70.1(1)–72.0(1)	N(1)–Sn(1)–C(10a)	91.4(8)–101.0(3)
O(1)–Sn(1)–C(10a)	81.7(6)–87.5(2)	N(1)–Sn(1)–C(14a)	91.9(4)–100.5(5)
O(1)–Sn(1)–C(14a)	84.1(2)–87.2(2)	C(10a)–Sn(1)–C(14a)	153(1)–168(1)
O(3)–Sn(1)–O(7)	123.0(1)–132.6(1)	Sn(1)–O(1)–C(1)	117.4(3)–120.5(3)
O(3)–Sn(1)–O(8)	74.8(1)–84.8(2)	Sn(1)–O(1)–Sn(2)	157.6(2)–165.8(2)
O(3)–Sn(1)–N(1)	79.9(2)–82.7(2)	Sn(1)–O(3)–C(9)	128.4(3)–135.1(4)
O(3)–Sn(1)–C(10a)	93.8(8)–103(1)	C(1)–O(1)–Sn(2)	76.8(3)–82.7(3)
O(3)–Sn(1)–C(14a)	94.3(7)–103.7(7)	O(1)–C(1)–O(2)	122.5(5)–124.8(5)
O(7)–Sn(1)–O(8)	46.3(1)–49.0(1)	C(1)–O(2)–Sn(2)	106.3(3)–113.2(3)
O(7)–Sn(1)–N(1)	146.7(1)–155.0(1)	Sn(1)–N(1)–C(2)	116.2(3)–118.4(3)
O(7)–Sn(1)–C(10a)	74.9(2)–88(1)	Sn(1)–N(1)–C(3)	124.5(4)–127.4(4)
O(7)–Sn(1)–C(14a)	74.8(4)–87.8(2)	C(2)–N(1)–C(3)	115.0(5)–117.6(5)

[a] The entries give the range displayed by the six chemically equivalent, symmetry unique occurrences of each listed parameter in the structure.

could only be maintained by recording the data at 0 °C and this yielded the structure of form **4b**. It is not clear whether both polymorphs were present all along, or if the second polymorph formed spontaneously from the first upon standing, or if the polymorphs result from a temperature-dependent phase change. The destruction of the crystals when cooled suggests a phase change, although it is unclear why it was only once possible to obtain a low-temperature data set without severe crystal destruction.

In the crystal structure of **5**, the asymmetric unit contains one formula unit of the Ph_2SnL^3 complex, plus half of a benzene molecule, which sits about a crystallographic centre of inversion. The Sn-complex units are linked into a polymeric *cis*-bridged chain by a very weak $Sn\cdots O(2)^i$ (symmetry operation i = 0.5 − *x*, 0.5 + *y*, 1.5 − *z*) interaction of 3.491(2) Å (Table 4) involving the Sn atom and the exocyclic carboxylate carbonyl O atom of the tridentate ligand of a neighboring Sn-complex unit (Fig. 7). The chain propagates in the crystallographic [0 1 0] direction. Without considering the weak $Sn\cdots O$ interaction, the Sn atom has a slightly distorted trigonal bipyramidal coordination geometry with the two O atoms of the tridentate aminoacetate ligand in axial positions (O(1)–Sn–O(3) = 161.21(8)°), and the coordination geometry is comparable with that observed in diphenyltin compounds of cognate systems [3,4]. When the additional long contact is considered, the coordination geometry becomes that of a rather distorted octahedron in which the long $Sn\cdots O$ contact is almost *trans* to one of the phenyl groups.

In the adduct between Ph_2SnL^2 and Phen (**6**), the Phen moiety coordinates to the Sn atom through Sn–N bonds that are approximately 0.4 Å longer than normally found for Sn–N bonds in aminostannate complexes (Fig. 8, Table 5). This may be a consequence of weak adduct formation, or steric repulsion between Phen and the coordinating O atoms of the aminoacetate ligand, which all lie roughly in the same plane. If the Phen coordination is ignored, the Sn atom coordination geometry of the diphenyltin complex is a quite distorted trigonal bipyramidal, particularly in the equatorial plane, with the phenoxide and carboxylic acid oxygen atoms of the aminoacetate ligand defining the axial positions (O1–Sn–O3 = 149.87(6)°). The geometry may even be considered as approaching that of a square pyramid, with the imino N atom in an apical position. In the structure of the parent Ph_2SnL^2 complex, which has a less distorted trigonal bipyramidal geometry, the axial O–Sn–O bond angles are around 160° [3], and a comparable bond angle is also present in compound **5** (vide supra). In **6**, the lower value of the O1–Sn–O3 bond angle results from the coordination of the Phen moiety; considering this species as well, the Sn atom has a slightly distorted pentagonal bipyramidal geometry in which the phenyl groups occupy axial positions. As the two weakly coordinated N atoms of the Phen moiety result in a very acute $N\cdots Sn\cdots N$ bite angle, this ligand could be considered to be sharing a single coordination site, in which case an alternative description of the coordination geometry could be distorted octahedral.

3.3. Spectroscopy

Compounds **1**, **2** and **5** were characterized previously by means of microanalysis, IR, NMR (^{1}H, ^{13}C, [119]Sn), and [119]Sn Mössbauer (in the case of **1** and **2**) spectroscopy [5]. Compounds **3**, **4** and **6** were subjected to ^{1}H and ^{13}C NMR analyses and their chemical shift assignments were made from the multiplicity patterns and/or resonance intensities [3–5] and also by standard distortionless enhancement by polarization transfer (DEPT) experiments. The ^{1}H and ^{13}C NMR spectra of the compounds show the expected resonances and integration.

The [119]Sn solution and isotropic [117]Sn solid-state NMR chemical shifts of compounds **1–6** are summarized in Table 6. The chemical shift data for compounds

Table 5
Selected bond lengths (Å) and angles (°) for compound **6**

Sn–O(1)	2.192(2)	O(2)–C(1)	1.225(3)
Sn–O(3)	2.108(2)	O(3)–C(9)	1.329(3)
Sn–N(1)	2.318(2)	N(1)–C(2)	1.465(3)
Sn–C(10)	2.125(2)	N(1)–C(3)	1.294(3)
Sn–C(11)	2.132(2)	Sn–N(23)	2.610(2)
O(1)–C(1)	1.287(3)	Sn–N(34)	2.711(2)
O(1)–Sn–O(3)	149.87(6)	C(2)–N(1)–C(3)	119.4(3)
O(1)–Sn–N(1)	72.24(7)	O(1)–C(1)–O(2)	124.4(2)
O(1)–Sn–C(10)	92.92(8)	N(23)–Sn–O(1)	131.74(6)
O(1)–Sn–C(11)	90.07(8)	N(23)–Sn–O(3)	78.11(6)
O(3)–Sn–N(1)	78.08(6)	N(23)–Sn–N(1)	156.00(7)
O(3)–Sn–C(10)	94.79(8)	N(23)–Sn–C(10)	83.96(8)
O(3)–Sn–C(11)	88.76(8)	N(23)–Sn–C(11)	84.81(8)
N(1)–Sn–C(10)	95.05(8)	N(34)–Sn–O(1)	70.19(6)
N(1)–Sn–C(11)	97.65(8)	N(34)–Sn–O(3)	139.89(6)
C(10)–Sn–C(11)	167.27(9)	N(34)–Sn–N(1)	141.71(7)
Sn–O(1)–C(1)	122.5(2)	N(34)–Sn–C(10)	79.83(8)
Sn–O(3)–C(9)	126.2(2)	N(34)–Sn–C(11)	89.58(8)
Sn–N(1)–C(2)	112.6(2)	N(23)–Sn–N(34)	61.84(6)
Sn–N(1)–C(3)	127.9(2)		

Table 6
Solution and solid-state tin NMR data for compounds 1–6

Compounds	δ [119]Sn (CDCl$_3$ solution, ppm)	δ_{iso} [117]Sn solid state (ppm)
1	−175	−71, −141, −156, −351
2	−213	−370, −374, −380, −390
3	−193	−369, −375, −382, −393
4	−214	−402, −410
5	−353	[a]
6	−388	[a]

[a] No [117]Sn MAS or CP/MAS spectrum could be obtained, probably due to the presence of several polymorphs, all having a very large chemical shift anisotropy which cannot be simplified, even by spinning at 10,000 Hz.

1–4 in $CDCl_3$ suggest that in non-coordinating solvents all species are monomeric, with pentacoordinated tin atoms bound to two oxygen atoms, one nitrogen atom and two alkyl groups, since all chemical shifts appear in the typical range for a trigonal bipyramidal geometry [19]. The corresponding solid-state spectra display very broad anisotropy patterns of over 1000 ppm, revealing more than one isotropic chemical shift. For the dibutyl derivatives **2–4**, the isotropic chemical shift values, all in the region −370 to −410 ppm are about 200 ppm higher than those found in the solution data and suggest seven-coordinated tin atoms. This is in agreement with the results of the X-ray crystal structure determinations (vide supra), which indicate that in the solid state two additional coordination sites to those found in solution are occupied by the formation of cyclic trinuclear moieties (compounds **3** and **4**), or dimers with additional H_2O ligands (compound **2**). The small differences in [117]Sn chemical shifts are due to the slightly different chemical environments of the tin atom in the powdered sample. The dimethyltin derivative **1** shows a major [117]Sn signal with a comparable chemical shift (seven coordinated, due to dimer formation and water coordination, as in **2**), but also contributions that apparently arise from monomeric species (−150 ppm, pentacoordinated, as in solution) and also a species with even weaker ligand coordination (−71 ppm, probably also pentacoordinated). The latter might be due to structures missing a significant Sn ← N coordination, as suggested by the fact that the shielding caused by Sn ← N coordination is weaker in the solid state (−141, −156 ppm) than in $CDCl_3$ (−175 ppm). This indicates that the actual product, **1**, displays polymorphism and that the determined crystal structure is representative of just one polymorph.

The diphenyltin complex **5** displayed a [119]Sn chemical shift at −353 ppm in solution, which closely matches the shifts reported for diphenyltin complexes [3,5] that have five-coordinated Sn atoms in solution. This shift value testifies that the polymeric structure of **5**, revealed in the crystal structure, is also not retained in solution. On the other hand, compound **6** requires special consideration. Diphenyltin(IV) 2-{[(E)-1-(2-oxyphenyl)ethylidene]amino}acetate (starting tin compound for **6**) displays a sharp signal ^{119}Sn NMR at −352 ppm in solution, which is ascribed to a pentacoordinated Sn atom [3]. This signal is found to be shifted upfield to −388 ppm when the tin atom is complexed with Phen to give **6**. Although the observed [119]Sn chemical shift for **6** closely matches the shift reported for diphenyltin compounds with octahedral coordination geometry [20], the crystal structure determination revealed that the coordination geometry around the Sn atom in compound **6** is a distorted pentagonal bipyramid (vide supra). In general, the [119]Sn values in seven-coordinate compounds are more than 100 ppm upfield from those

in six-coordinate analogues [21]. The lower value of the chemical shift in **6** might be ascribed to the long Sn···N(phen) bonds (0.4 Å longer than normal Sn–N bonds). It is also possible that weak coordination of Phen to give two long Sn···N(phen) bonds may give a shift similar to that expected for one normal Sn–N bond. Thus, the ^{119}Sn NMR data are consistent with compound **6** having a seven-coordinate structure in solution.

ESI mass spectra were recorded for compounds **1–6**. First order mass spectra were used to confirm the molecular weights of the compounds, while tandem mass spectrometric measurements (MS^n) were used to verify the particular structural features [22–26]. Non-covalent complexes fragmented very easily and therefore the tuning parameter ''compound stability'' had to be reduced to 20% to observe the sodiated molecular adduct $[M + Na]^+$ essential for molecular weight determination. The typical ions in the first-order ESI mass spectra of **1–6** are adducts of monomeric and higher polymeric forms of the molecules with sodium or potassium ions and fragment ions formed by successive losses of monomeric units. The tandem mass spectra (MS/MS) confirm that this fragmentation contributes to the relative abundances of lower oligomeric ions in the first-order mass spectra, e.g., the MS/MS spectrum of $[M_{tri} + Na]^+$ yields $[M_{di} + Na]^+$, then the MS^3 spectrum of $[M_{di} + Na]^+$ yields $[M_{mono} + Na]^+$, and finally the MS^4 spectrum of $[M_{mono} + Na]^+$ gives other fragment ions, such as the neutral losses of butene, butane, etc. Moreover, the presence of more than one tin atom in the molecule causes a wide distribution of the total ion signal among many isotopes, which decreases the relative intensity of this centroid peak. This means that, in principle, all monomeric and dimeric ions observed in the first-order spectra of **1–6** may be formed by the fragmentation. Although the crystal structure shows the presence of a water ligand in **1**, the corresponding mass with the presence of coordinated water is not found in the mass spectra, which can be explained by the easy loss of neutral water during the ionization. The deprotonated molecule $[M − H]^-$ is the base peak of all first-order negative-ion spectra. In contrast to the positive-ion mode, the negative-ion spectra do not provide any information on the polymeric species. Therefore, the positive-ion ESI-MS is preferred for studying these polymeric organotin compounds. The neutral losses observed in the tandem mass spectra are in accordance with expected structures, such as CO_2, butene, butane, methanol, benzene, etc.

4. Supplementary material

CCDC-262053–CCDC-262059 contain the supplementary crystallographic data for complexes **1**, **2**, **3**, **4a**, **4b**, **5** and **6**, respectively. These data can be obtained

free of charge via www.ccdc.cam.ac.uk/conts/retriev-ing.html (or from the Cambridge Crystallographic Data Centre, 12 Union Road, Cambridge CB2 1EZ, UK; fax: +44 1223 336033; e-mail: deposit@ccdc.cam.ac.uk).

Acknowledgments

References

[1] E.R.T. Tiekink, Appl. Organomet. Chem. 5 (1991) 1;
    E.R.T. Tiekink, Trends Organomet. Chem. 1 (1994) 71.
[2] M. Gielen, Coord. Chem. Rev. 15 (1996) 41;
    D. de Vos, R. Willem, M. Gielen, K.E. van Wingerden, K. Nooter, Metal-Based Drugs 5 (1998) 179;
    M. Kemmer, M. Gielen, M. Biesemans, D. de Vos, R. Willem, Metal-Based Drugs 5 (1998) 189;
    M. Gielen, E.R.T. Tiekink, in: M. Gielen, E.R.T. Tiekink (Eds.), Metallotherapeutic Drug and Metal-based Diagnostic Agents: ^{50}Sn Tin Compounds and Their Therapeutic Potential, Wiley, 2005, pp. 421–439 (Chapter 22).
[3] D. Dakternieks, T.S. Basu Baul, S. Dutta, E.R.T. Tiekink, Organometallics 17 (1998) 3058.
[4] T.S. Basu Baul, E.R.T. Tiekink, Z. Kristallogr. NCS 214 (1999) 361.
[5] T.S. Basu Baul, S. Dutta, E. Rivarola, M. Scopelliti, S. Choudhuri, Appl. Organomet. Chem. 15 (2001) 947.
[6] T.S. Basu Baul, S. Dutta, E. Rivarola, R. Butcher, F.E. Smith, J. Organomet. Chem. 654 (2002) 100.
[7] T.S. Basu Baul, S. Dutta, C. Masharing, E. Rivarola, U. Englert, Heteroatom. Chem. 14 (2003) 149.
[8] T.S. Basu Baul, D. de Vos, unpublished results.
[9] R. Hooft, KappaCCD Collect Software, Nonius BV, Delft, The Netherlands, 1999.
[10] Z. Otwinowski, W. Minor, in: C.W. Carter Jr., R.M. Sweet (Eds.), Methods in Enzymology, vol. 276, Macromolecular Crystallography, Part A, Academic Press, New York, 1997, pp. 307–326.
[11] R.H. Blessing, Acta Crystallogr., Sect. A 51 (1995) 33.
[12] G.M. Sheldrick, SHELXS97, Program for the Solution of Crystal Structures, University of Göttingen, Germany, 1997.
[13] A. Altomare, G. Cascarano, C. Giacovazzo, A. Guagliardi, M.C. Burla, G. Polidori, M. Camalli SIR92, J. Appl. Crystallogr. 27 (1994) 435.
[14] A.L. Spek, PLATON, Program for the Analysis of Molecular Geometry, University of Utrecht, The Netherlands, 2004.
[15] P. van der Sluis, A.L. Spek, Acta Crystallogr., Sect. A 46 (1990) 194.
[16] H.D. Flack, G. Bernardinelli, Acta Crystallogr., Sect. A 55 (1999) 908;
    H.D. Flack, G. Bernardinelli, J. Appl. Crystallogr. 33 (2000) 1143.
[17] G.M. Sheldrick, SHELXL97, Program for the Refinement of Crystal Structures, University of Göttingen, Germany, 1997.
[18] J. Bernstein, R.E. Davis, L. Shimoni, N.-L. Chang, Angew. Chem. Int. Ed. Engl. 34 (1995) 1555.
[19] J. Holeček, M. Nádvorník, K. Handlíř, A. Lyčka, J. Organomet. Chem. 315 (1986) 299.
[20] J. Otera, J. Organomet. Chem. 221 (1981) 57.
[21] J. Otera, T. Hinoishi, R. Okawara, J. Organomet. Chem. 202 (1980) C93.
[22] C.L. Gatlin, F. Tureček, in: R.B. Cole (Ed.), Electrospray Ionization of Inorganic and Organometallic Complexes, in Electrospray Ionization Mass Spectrometry: Fundamentals, Instrumentation and Applications, Wiley, New York, 1997, pp. 527–570.
[23] A. Růžička, L. Dostál, R. Jambor, V. Buchta, J. Brus, I. Císařová, M. Holčapek, J. Holeček, Appl. Organomet. Chem. 16 (2002) 315.
[24] R. Jambor, L. Dostál, A. Růžička, I. Císařová, J. Brus, M. Holčapek, J. Holeček, Organometallics 21 (2002) 3996.
[25] A. Růžička, A. Lyčka, R. Jambor, P. Novák, I. Císařová, M. Holčapek, M. Erben, J. Holeček, Appl. Organomet. Chem. 17 (2003) 168.
[26] L. Kolářová, M. Holčapek, R. Jambor, L. Dostál, A. Růžička, M. Nádvorník, J. Mass Spectrom. 39 (2004) 621.